Submitted to Journal of Spacecraft and Rockets
Log No: A10874
Date Logged: 26 April 1999

Application of Energy Storage To Solar Electric Propulsion Orbital Transfer*

Mark W. Marasch† and Christopher D. Hall‡

Abstract

Solar electric propulsion uses solar panels to generate power for electric thrusters. Using stored energy makes it possible to thrust through eclipses, but requires that some of the solar power collected during the sunlit portion of the trajectory be used to recharge the storage system. Previous researchers have reported that the required energy storage mass can be prohibitive. However, the use of high-speed flywheels for energy storage can provide advantages. In this paper, we compare the effectiveness of orbit transfers using and without using energy storage. The orbit transfers are developed as sequences of time-optimal circle-to-circle planar transfers from low-Earth orbit to geostationary orbit. We develop techniques for solving the appropriate boundary value problems, and illustrate tradeoffs between solar array and flywheel-battery masses for transfers

* Presented at the 1998 AAS/AIAA Space Flight Mechanics Meeting, Monterey, California, as Paper AAS 98-204.

†Graduate student, Department of Aeronautics and Astronautics, Air Force Institute of Technology, Wright-Patterson Air Force Base, Ohio. Currently Captain, USAF, Air Force Research Laboratory, AFRL/VSDD, 3550 Aberdeen SE, Kirtland Air Force Base, New Mexico 87117

‡Assistant Professor, Aerospace and Ocean Engineering, Virginia Polytechnic Institute and State University, Blacksburg, Virginia 24061-0203. Associate Fellow AIAA.

requiring multiple revolutions. The utility of flywheel energy storage specifically for the use of the solar electric propulsion system is examined. We find that when flywheel energy storage is used in these scenarios, transit times are typically increased, but significant propellant mass savings can be realized. Furthermore, if the spacecraft has a requirement for energy storage, then it is advantageous to use stored energy during the orbit transfer.

Nomenclature

a	=	acceleration (m/s^2)
D	=	difference between collected energy and energy storage capacity (W-hr)
F	=	fraction of power applied to power available
G	=	excess energy (W-hr)
g_0	=	gravitational acceleration at the Earth's surface (km/s^2)
m	=	mass (kg)
$\dot{m}$	=	mass flow rate (kg/s^2)
P_a	=	power applied to thruster (W)
P_e	=	power available from solar array (W)
P_L	=	power required by payload (W)
r	=	distance between spacecraft and the Earth's center (km)
$r_\oplus$	=	radius of the Earth (km)
t	=	time (s)
t_f	=	time of flight (s)
t_{orb}	=	orbital period (s)
t_{sh}	=	time spent in shadow (s)
t_{sun}	=	time spent in sunlight (s)
T	=	thrust (N)
u	=	radial component of velocity (km/s)
v	=	transverse component of velocity (km/s)

α = shadow geometry angle (rad)

β = energy density (W-hr/kg)

ϕ = angle between thrust direction and local horizontal (rad)

γ = shadow half-angle (rad)

η = engine efficiency

λ_r = costate for radius

λ_u = costate for radial velocity component

λ_v = costate for transverse velocity component

μ = gravitational parameter

θ = angular measure of spacecraft position (rad)

Introduction

Solar electric propulsion (SEP) is an effective technology for transferring a satellite from an initial low-Earth orbit (LEO) to a higher altitude operational orbit such as a geostationary orbit (GEO). One drawback to SEP is the loss of solar panel power when the spacecraft is in eclipse. In the worst case of a transfer in the ecliptic plane, the vehicle will experience eclipse on every revolution, with the eclipse duration increasing and the fraction of the orbit spent in eclipse decreasing as radius increases. One approach to dealing with this situation is to coast through the eclipses. It is also possible to use plane changes to reduce eclipse duration, but plane changes require significant propellant usage.

Kechichian[1] discussed in detail the problems associated with the Earth's shadow and continuous low-thrust orbit transfers. In Ref. 1, he developed an orbit predictor for tangential thrust that takes into account the effects of coasting through the eclipses. He also discussed the effectiveness of constraining the individual revolutions to be circular

orbits. Kluever and Oleson[2] developed a direct method for obtaining nearly optimal LEO to GEO transfers. Free[3] studied the use of electric propulsion for stationkeeping for GEO satellites, including the use of energy storage during eclipse.

Another approach for orbital transfer is to use energy storage to thrust continuously through the eclipses. Thrusting through eclipse requires using some of the available solar panel power to charge the energy storage system, thus reducing the power and thrust during the sunlit portion of each revolution. This concept has been explored by Avila[4] and by Fitzgerald.[5] Avila[4] pointed out that, if conventional battery systems are used, the mass required to run thrusters in eclipse is prohibitively large. Fitzgerald[5] also addressed the issue of SEP and energy storage, and reached the same conclusion. Fitzgerald examined how adding batteries to a solar electric propulsion system can assist in decreasing the transit time to a higher Earth orbit, by allowing thrusters to be run in eclipse. The results showed that the advantage gained in terms of transit time is far outweighed by the increase in system mass. However, Fitzgerald did not use optimal transfers and used conventional batteries with low energy density.

In this paper, we reexamine the question of whether energy storage can be used to improve the performance of SEP for orbit transfer. Flywheel energy storage (FES) systems have several potential advantages over conventional chemical batteries. The potential advantages most relevant to the application presented here are increased depth of discharge and increased energy density. Because the energy is stored mechanically, the allowable depth of discharge of FES may as large as 90%, and will certainly be larger than the 30% typical of chemical batteries. Furthermore, the energy density of FES may also exceed that for chemical batteries. Although there are many technical challenges to the implementation of this technology, energy densities of up to 100–300 W-hr/kg have been projected.[6,7] Another advantage of FES systems is that the flywheels may also be used to control the attitude of the spacecraft; this advantage

is not discussed further here.[8–10]

We combine the subjects of solar electric propulsion, optimal orbital transfer and flywheel energy storage. By combining optimal orbital transfers with the specific energies that FES may provide, we show that energy storage may be useful for SEP systems.

We begin by stating the equations of motion for time-optimal planar orbital transfers, and describing results that have been previously developed for numerically obtaining optimal solutions. We then describe our approach to applying these solutions to the specific problem of orbital transfer using energy storage. We present results in order to answer two basic questions: i) is it advantageous to use existing energy storage to thrust through eclipse? and ii) is it more advantageous to add solar panel mass or storage system mass? In the former case, we can definitely answer in the affirmative, and in the latter, the answer depends on the relationship between the power density of the solar panels and the energy density of the storage system.

Optimal Continuous-Thrust Orbit Transfer

The approach developed here is based on minimum-time, continuous-thrust, coplanar orbit transfers with circular boundary conditions. The theory for time-optimal transfers is well-known, with prior sources given in Refs. 11 and 12. These two papers also develop the state and costate equations of motion used in the present paper, as well as initial costate approximations that are used here. The variables involved are shown in Fig. 1.

Equations 1–8 define the time-optimal orbit transfer problem. These equations describe minimum-time, constant-thrust, planar orbital transfers in polar coordinates. For this case, the propulsion system runs at its full capacity. The thrust magnitude, T, and the mass flow rate, $\dot{m}$, are known. The variable r is the spacecraft's distance

from the center of the primary body, u is the radial component of velocity, and v is the transverse component of velocity; the corresponding equations are Eqs. 1–3. The variables λ_r, λ_u, and λ_v are the costates corresponding to radius, radial velocity, and transverse velocity, with equations of motion in Eqs. 4–6. The thrust acceleration $a(t)$ is defined by Eq. 7 and the optimal thrust angle ϕ is given by Eq. 8.

$$\dot{r} = u \tag{1}$$

$$\dot{u} = \frac{v^2}{r} - \frac{\mu}{r^2} + a(t)\sin\phi \tag{2}$$

$$\dot{v} = -\frac{uv}{r} + a(t)\cos\phi \tag{3}$$

$$\dot{\lambda}_r = -\lambda_u\left(-\frac{v^2}{r^2} + \frac{2\mu}{r^3}\right) - \lambda_v\frac{uv}{r^2} \tag{4}$$

$$\dot{\lambda}_u = -\lambda_r + \lambda_v\frac{v}{r} \tag{5}$$

$$\dot{\lambda}_v = -\lambda_u\frac{2v}{r} + \lambda_v\frac{u}{r} \tag{6}$$

$$a(t) = \frac{T}{m(0) - \dot{m}t} \tag{7}$$

$$\phi = \tan^{-1}\left(\frac{\lambda_u}{\lambda_v}\right) \tag{8}$$

In general, an orbit transfer begins with known initial conditions and desired final conditions for the states r, u, and v, but neither the initial nor the final values of the costates are known. The central problem in solving optimal control problems of this form is solving the boundary-value problem (BVP) to find the initial values of the costates that lead to the desired final values of the states. For example, for a planar, circle-to-circle transfer, the boundary conditions are as given in Table 1. Solving the boundary value problem requires initial estimates of the costates $\lambda_r(0)$, $\lambda_u(0)$, $\lambda_v(0)$, and of the time-of-flight, t_f. As described in Ref. 11, the costate initial conditions can be scaled so that $\lambda_r(0) = 1$. Then, for low thrust, good initial estimates for the remaining variables are $\lambda_u(0) = 0$, $\lambda_v(0) = 1$, and $t_f = (1 - 1/\sqrt{R})/a(0)$, where R is the final radius of the transfer. We then use the shooting method, with quasi-Newton

iteration to obtain the optimal solution. For this problem, the quasi-Newton iteration step is typically of the form:

$$\begin{bmatrix} \Delta t_f \\ \Delta\lambda_u(0) \\ \Delta\lambda_v(0) \end{bmatrix} = \begin{bmatrix} \frac{\partial r(t_f)}{\partial t_f} & \frac{\partial r(t_f)}{\partial \lambda_u(0)} & \frac{\partial r(t_f)}{\partial \lambda_v(0)} \\ \frac{\partial u(t_f)}{\partial t_f} & \frac{\partial u(t_f)}{\partial \lambda_u(0)} & \frac{\partial u(t_f)}{\partial \lambda_v(0)} \\ \frac{\partial v(t_f)}{\partial t_f} & \frac{\partial v(t_f)}{\partial \lambda_u(0)} & \frac{\partial v(t_f)}{\partial \lambda_v(0)} \end{bmatrix}^{-1} \begin{bmatrix} \Delta r(t_f) \\ \Delta u(t_f) \\ \Delta v(t_f) \end{bmatrix} \tag{9}$$

where the errors $\Delta r(t_f)$, $\Delta u(t_f)$, and $\Delta v(t_f)$ are the differences between the current final values and the desired final values, and Δt_f, $\Delta\lambda_u(0)$, and $\Delta\lambda_v(0)$ are the refinements to be subtracted from the previous estimates. This iteration continues until the errors are reduced to a desired tolerance. All results reported here use a tolerance where the norm of the error is $< 10^{-8}$. As described in Ref. 12, a step-limiting procedure is used to improve convergence.

Each transfer segment described by these equations uses a fixed thrust magnitude, and achieves a transfer in minimum time by continuously varying ϕ, the direction in which thrust is applied. For a continuous-thrust transfer with constant thrust, the trajectory that minimizes time in transit also minimizes the propellant used.

Before proceeding with the development, a discussion of the scope of this paper is needed. The problem of interest is to determine the possible advantages of using energy storage to thrust through eclipses. Eclipses can be partially avoided by changing the osculating plane of the orbit during the transfer, thereby improving the performance of SEP without using energy storage. Allowing the instantaneous eccentricity to increase during the transfer may also lead to improved performance. There is also a penalty for slow transit of the van Allen belts due to the degradation of solar cells caused by radiation, so that passing quickly through these altitudes is also important. These approaches are certainly of interest and their effects should be investigated in future studies; however, in order to focus on the effects of energy storage, we limit the present investigation as follows. Instead of allowing the inclination to vary, we restrict the

entire orbit transfer to the plane of the ecliptic. While this differs from what would be done in practice, it provides the worst possible case for eclipse duration. If the inclination were allowed to vary, we believe that the qualitative results reported here would still be valid. Instead of allowing a completely general planar transfer from LEO to GEO, we divide the transfer into a sequence of single-orbit transfers with circular boundary conditions. While this almost certainly does not provide the truly time-optimal solution, it allows a straightforward comparison of the transfers using energy storage with those that coast through the eclipses. In the subsequent section we describe the four possible cases for the individual transfer segments.

LEO-to-GEO Modeling Approach

If we consider a continuous transfer from LEO to GEO, then only one BVP must be solved. However, for low thrust levels ($T/W_0 \approx 10^{-4}$), convergence is sensitive to small changes in the initial costates due to the numerous revolutions required to reach the higher orbit. Furthermore, we want to include the possibility of coasting through eclipse, which gives a discontinuous thrust profile. For these problems, one may apply orbital averaging or direct optimization methods (*e.g.*, Kluever and Oleson[2]). Ideally, one would seek the minimum-time or minimum-fuel trajectory from LEO to GEO, allowing three-dimensional changes in the trajectory.

However, since we are primarily interested in the possible advantage of using energy storage during eclipse, It is well-known that the thrust angle is nearly zero (*i.e.*, tangential steering) as thrust approaches zero and that the osculating orbit is nearly circular.

We examine orbital transfers that take many revolutions to complete. We break large transfers into single revolution segments. Each segment begins as the spacecraft leaves the Earth's shadow, and is an optimal, planar, constant-thrust, circle-to-circle

transfer. If a spacecraft has no capacity to store energy for propulsion, each transfer segment must be completed when it returns to the Earth's shadow. When the spacecraft has some energy storage capacity, these transfer segments are allowed to continue into the Earth's shadow until the stored energy is exhausted. When a spacecraft has enough energy storage to continue thruster operation through the Earth's shadow, continuous transfers become possible. All of the trajectories in this paper are described by the same equations of motion, but each of the described cases presents a different boundary value problem to be solved.

All of the orbital transfers to be modeled are planar and in the ecliptic plane. This assumption has the effect of maximizing time in eclipse for any orbital radius, providing the worst possible scenario for solar electric propulsion. A cylindrical approximation is used for the Earth's shadow, as shown in Fig. 2. Using this geometry, the angular portion of a circular orbit spent in shade is 2γ, where

$$\gamma = \sin^{-1}\left(\frac{r_\oplus}{r}\right) \tag{10}$$

$r_\oplus$ is the Earth's radius, and r is the radius of the orbit. For a more accurate model of shadow geometry, see Ref. 13.

Case One: Circle-to-Circle Transfer Segments Without Shade Constraints

When $r(t_f) - r(0)$ is "small," the transfer can be accomplished without entering the Earth's shadow, and we refer to this as Case 1. Figure 3 illustrates the concept of such a transfer, with dashed lines indicating the Earth's shadow, concentric circles depicting two circular orbits, and the arc connecting them representing the transfer. This is the same problem as treated in Thorne and Hall.[12] This is a minimum-time transfer, and the appropriate Newton step for solving the boundary-value problem is given by Eq. 9.

Case Two: Transfer Segments Without Energy Storage

For the second case, no energy storage is used and we wish to maximize the radius increase achieved during each period of sunlight. Integration is carried out using the same equations of motion used for Case 1, but the boundary value problem to be solved is different. As illustrated in Fig. 4, this transfer is maximized when the entire period spent in sunlight is used to complete the transfer. Note that the transfer is shown to begin just as the spacecraft exits the Earth's shadow, and ends just as it enters eclipse again.

In order for the transfer segment to end just as the spacecraft enters eclipse, the $r(t_f)$ requirement of Case 1 is replaced by the angle requirement:

$$\theta(t_f) = 2\pi - \sin^{-1}\left(\frac{r_\oplus}{r(0)}\right) - \sin^{-1}\left(\frac{r_\oplus}{r(t_f)}\right) \tag{11}$$

where $\theta(t_f)$ is the angle swept out by the spacecraft in the transfer segment. Here the problem is to maximize the final radius achieved in sunlight. By replacing each occurrence of $r(t_f)$ in Eq. 9 with $\theta(t_f)$, we create Newton steps that lead to solving this problem directly.

$$\begin{bmatrix} \Delta t_f \\ \Delta\lambda_u(0) \\ \Delta\lambda_v(0) \end{bmatrix} = \begin{bmatrix} \frac{\partial\theta(t_f)}{\partial t_f} & \frac{\partial\theta(t_f)}{\partial\lambda_u(0)} & \frac{\partial\theta(t_f)}{\partial\lambda_v(0)} \\ \frac{\partial u(t_f)}{\partial t_f} & \frac{\partial u(t_f)}{\partial\lambda_u(0)} & \frac{\partial u(t_f)}{\partial\lambda_v(0)} \\ \frac{\partial v(t_f)}{\partial t_f} & \frac{\partial v(t_f)}{\partial\lambda_u(0)} & \frac{\partial v(t_f)}{\partial\lambda_v(0)} \end{bmatrix}^{-1} \begin{bmatrix} \Delta\theta(t_f) \\ \Delta u(t_f) \\ \Delta v(t_f) \end{bmatrix} \tag{12}$$

Case Three: Low Levels of Energy Storage

A spacecraft may have some energy storage, but not enough to continue thruster operation through the entire eclipse. Under these circumstances, a circle-to-circle transfer is performed as illustrated in Fig. 5. Here, the spacecraft begins a transfer segment as it leaves the Earth's shadow and completes a circle-to-circle transfer just as the stored energy is depleted.

With the use of energy storage, budgeting energy is a concern. If all of the power received by the solar array is sent directly to the thrusters, there is no stored energy to

use in eclipse. However, we may choose to channel just enough power to the flywheel batteries to provide a full charge at the moment the spacecraft enters eclipse. The remaining power is used to run the thrusters in sunlight. The thrusters continue to run at the same level in eclipse, until the energy supply is exhausted. Because the thrusters are not operated at full capacity, we assume that mass flow rates and thrust are proportional to the power consumed.

When in sunlight, the spacecraft has a fixed value of available power from the solar array, P_e, and we must determine the level of power that is actually applied to the thrusters, P_a. We define a power fraction, F, by

$$F = P_a/P_e \tag{13}$$

We need to find t_f, λ_u, λ_v, and F that satisfy the boundary conditions. The need to budget energy results in two new constraints. The first is the requirement that the energy used is exactly the energy that is collected by the solar array (assuming 100% storage and conversion efficiency):

$$P_a t_f = P_e t_{sun} \Rightarrow F t_f = t_{sun} \tag{14}$$

In this equation, t_{sun} is the period of time spent in sunlight. This condition must be met, as the spacecraft can not use more energy than its array collects. Also, if any of the collected energy is not used, the system performance is suboptimal. We define an energy excess variable, G, by

$$G = P_e t_{sun} - P_a t_f = P_e(t_{sun} - F t_f) \tag{15}$$

A positive value of G represents excess energy that is not used. A negative value of G is an energy deficit. To satisfy Eq. 14, the value of G should be zero.

The second constraint to be enforced is that the battery must be fully charged just

as the spacecraft enters the Earth's shadow, meaning:

$$m_{fb}\beta = (P_e - P_a)t_{sun} \tag{16}$$

where m_{fb} is the mass of the flywheel-battery system, and β is the usable energy density. If, for instance, we have 100 W-hr/kg flywheel batteries designed for up to a 90% depth of discharge, then $\beta = 90$ W-hr/kg. We use D to represent the difference between battery charge and capacity:

$$D = (P_e - P_a)t_{sun} = P_e(1 - F) - m_{fb}\beta \tag{17}$$

To satisfy Eq. 16, $D = 0$ is required.

This is a 4×4 problem where the Δr achieved in one revolution is maximized. The Newton steps are calculated as:

$$\begin{bmatrix} \Delta t_f \\ \Delta\lambda_u(0) \\ \Delta\lambda_v(0) \\ \Delta F \end{bmatrix} = \begin{bmatrix} \frac{\partial D}{\partial t_f} & \frac{\partial D}{\partial \lambda_u(0)} & \frac{\partial D}{\partial \lambda_v(0)} & \frac{\partial D}{\partial F} \\ \frac{\partial u(t_f)}{\partial t_f} & \frac{\partial u(t_f)}{\partial \lambda_u(0)} & \frac{\partial u(t_f)}{\partial \lambda_v(0)} & \frac{\partial u(t_f)}{\partial F} \\ \frac{\partial v(t_f)}{\partial t_f} & \frac{\partial v(t_f)}{\partial \lambda_u(0)} & \frac{\partial v(t_f)}{\partial \lambda_v(0)} & \frac{\partial v(t_f)}{\partial F} \\ \frac{\partial G}{\partial t_f} & \frac{\partial G}{\partial \lambda_u(0)} & \frac{\partial G}{\partial \lambda_v(0)} & \frac{\partial G}{\partial F} \end{bmatrix}^{-1} \begin{bmatrix} \Delta D \\ \Delta u(t_f) \\ \Delta v(t_f) \\ \Delta G \end{bmatrix} \tag{18}$$

Computational experience has shown that the iteration converges to a solution using simple low-thrust assumptions.

Case Four: High Levels of Energy Storage

Case 4 is similar to Case 3, in that energy storage is used to continue thruster operation in eclipse, and the Δr achieved in one revolution is maximized. The difference is that enough energy storage capacity is available to run the thrusters completely through the Earth's shadow. An example transfer segment is shown in Fig. 6. Here, the spacecraft begins a transfer as it leaves the Earth's shadow, and completes a circle-to-circle transfer just as it is about to leave the Earth's shadow again. The constraints for

this problem are similar to those in Case 3, but the charge constraint D disappears. The charge constraint is replaced by the angle constraint:

$$\theta(t_f) = 2\pi - \sin^{-1}\left(\frac{r_\oplus}{r(0)}\right) + \sin^{-1}\left(\frac{r_\oplus}{r(t_f)}\right) \tag{19}$$

Beyond this one change, we have a problem similar to Case 3. One step in the Newton iteration is performed as:

$$\begin{bmatrix} \Delta t_f \\ \Delta\lambda_u(0) \\ \Delta\lambda_v(0) \\ \Delta F \end{bmatrix} = \begin{bmatrix} \frac{\partial\theta(t_f)}{\partial t_f} & \frac{\partial\theta(t_f)}{\partial\lambda_u(0)} & \frac{\partial\theta(t_f)}{\partial\lambda_v(0)} & \frac{\partial\theta(t_f)}{\partial F} \\ \frac{\partial u(t_f)}{\partial t_f} & \frac{\partial u(t_f)}{\partial\lambda_u(0)} & \frac{\partial u(t_f)}{\partial\lambda_v(0)} & \frac{\partial u(t_f)}{\partial F} \\ \frac{\partial v(t_f)}{\partial t_f} & \frac{\partial v(t_f)}{\partial\lambda_u(0)} & \frac{\partial v(t_f)}{\partial\lambda_v(0)} & \frac{\partial v(t_f)}{\partial F} \\ \frac{\partial G}{\partial t_f} & \frac{\partial G}{\partial\lambda_u(0)} & \frac{\partial G}{\partial\lambda_v(0)} & \frac{\partial G}{\partial F} \end{bmatrix}^{-1} \begin{bmatrix} \Delta\theta(t_f) \\ \Delta u(t_f) \\ \Delta v(t_f) \\ \Delta G \end{bmatrix} \tag{20}$$

This maneuver is enabled by sufficient energy storage. If there is any doubt about whether or not the on-board battery capacity is adequate, it can be checked after the problem is solved. This check is accomplished by finding the shadow-crossing time, t_{sc}, and ensuring that the following condition is met:

$$P_a(t_f - t_{sc}) \leq m_{fb}\beta \tag{21}$$

If the condition of Eq. 21 is not met, Case 4 is not the appropriate case, and Case 3 should be used to obtain a maximum radius increase for this transfer segment.

In this section, we have developed the tools necessary to propagate optimal orbital transfer segments. Techniques for solving the boundary value problems for a number of different schemes have been developed. By piecing together a number of such segments, large orbital transfers can be accomplished. In the sections to follow, these tools are used to determine what advantages flywheel energy storage can yield.

A flowchart of the algorithm used to propagate large orbital transfers is displayed in Fig. 7. For each transfer segment, the appropriate routine is called to solve the boundary value problem. If there is some question about which case should be solved for a given transfer segment, Fig. 8 illustrates the process used to select the best one.

Results Using Energy Storage

In this section, we use these techniques to examine the benefits of energy storage applied to solar electric orbital transfers. Initially, we analyze the concept of adding energy storage solely for use by the solar electric propulsion system, ignoring the fact that most satellites have storage needs for their on-orbit missions, and examine the resulting mass tradeoff. In Ref. 14, tradeoffs are examined for single-segment trajectories. In order to conserve space, this analysis has been omitted. Instead, we analyze large-scale orbital maneuvers using the techniques described in the previous section. Then we consider the more relevant case of a satellite that already has an energy storage system.

Energy Storage Strictly for Propulsion

The problem is initialized as a 3000 kg spacecraft in a circular parking orbit with a 250 km altitude. We use a Hall-effect thruster that provides 0.06118 N/kW and has a mass flow rate of 3.899 $\times 10^{-6}$ kg/(s kW). The initial thrust-to-weight ratio is approximately 1.8×10^{-4}, and the initial I_{sp} is approximately 1600. We assume a usable battery energy density of 100 W-hr/kg, and an array specific power of 120 W/kg. Two transfers are propagated, one without storage and one with a degree of storage optimized for the highest performance at low altitude from Ref. 14. Both systems have a total array and battery mass of 717 kg. For the transfer without storage, the array is 717 kg. For the case with storage, the array mass is 522 kg and the flywheel-battery mass is 195 kg.

Figure 9 illustrates radius with respect to time for the two systems being compared. Note that both systems overshoot the geosynchronous target ($r = 42,164$ km), because the algorithm designed to achieve the correct final radius is not implemented for this comparison. The reason the correct algorithm is not implemented in this example is

because it is not needed for this comparison. Toward the end of these transfers, the increases made by individual transfer segments are several thousand kilometers apiece. Though exact ending of the transfers is not modeled in this example, the trends are clear: the spacecraft that does not use stored energy reaches geosynchronous orbit first. Figure 10 is a magnified view of the radius versus time results for the first 15 days. Note that the spacecraft with storage is ahead until some point after a radius of 8000 km. The time spent getting to the final orbit is not the only matter of interest, though. We are also interested in which system makes the most efficient use of propellant mass.

Figure 11 shows the results when we plot remaining spacecraft mass against achieved radius. The system that used energy storage takes longer, but realizes a great benefit with respect to the mass of the payload that can be delivered to any altitude. The payload mass delivered to GEO by the system using energy storage is approximately 100 kg larger, though it takes about 10 days longer to get there. Recall that the flywheel-battery mass does not encroach on the payload mass, because the total flywheel-battery and array mass is equal to the array mass for the case without storage. Several similar comparisons have been run, and this trend is consistently observed.[14]

We have compared a system using no storage to a system of equal mass, with some of its array mass replaced with a flywheel-battery system. The results show that the system with flywheel storage takes longer to reach a geosynchronous orbit, but does so more efficiently in terms of propellant usage. In this analysis, we have ignored the fact that most spacecraft have on-orbit energy storage needs. Next we discuss optimizing systems which have some minimum energy storage and power requirements for their on-orbit missions.

Energy Storage for On-Orbit Mission Requirements

For this analysis, we allow no additional array or battery mass beyond what is necessary

to meet on-orbit mission requirements. Then, we analyze the performance of the same spacecraft, but with additional mass allotted for array and battery. The additional mass can be distributed as array, battery, or a combination, and we investigate the effect of this distribution on performance in terms of transfer time and propellant used.

We begin with a spacecraft with some high power requirements for its on-orbit mission in a geosynchronous orbit. Because this spacecraft must not cease operation when it passes through the Earth's shadow, it has a requirement for energy storage. We assume that all of the power provided by the solar array can be used for propulsion during the spacecraft's LEO to GEO transfer, and that we are not allowed to carry any additional mass for a larger array or battery to use for this transfer. There are two extreme approaches that can be used to perform this transfer. The spacecraft can rely on its panels alone and coast through eclipses, or it can use its battery storage capacity and perform a transfer without any coast periods.

The spacecraft has a parking-orbit mass of 3000 kg, and a payload power requirement of 10 kW. During the period when a satellite at this altitude would have maximum eclipse, we know that the following power balance must be met:

$$P_e t_{sun} = P_L t_{orb} \tag{22}$$

Here P_e is the power available from the solar array, t_{sun} is the period of sunlight in one orbit, P_L is the payload's power requirement, and t_{orb} is the period of one orbit. To meet the worst-case eclipse conditions for GEO, the panels must be capable of collecting excess power that can be saved for use in eclipse, which leads to $P_e \approx 10.5$ kW for the 10 kW payload. If the arrays have a specific power of 120 W/kg, then the array mass is 87.5 kg. The capacity of the battery system must satisfy

$$m_{fb}\beta = P_L t_{sh} \tag{23}$$

where m_{fb} is the battery mass, β is the usable energy density, and t_{sh} is the maximum period spent in eclipse ($T_{sh} \approx 1.16$ hours for GEO). Using this relationship, and the value $\beta = 100$ W-hr/kg, we find that the minimum battery mass is 116 kg for a 10 kW payload in GEO.

The algorithm used for these transfers is the same as the one illustrated in Fig. 7. The difference lies in the choice of the appropriate boundary value problem to solve. We are comparing a transfer where the flywheel-batteries are used to a transfer where they are not. For the first trial an orbital transfer based on the Case 2 boundary value problem is propagated, where no energy storage is used. For the second transfer, Case 4 is used. Because the energy storage available is designed for an eclipse situation found at GEO, the last maximum increase segment is the only one that is likely to come close to using the entire capacity of the battery system. Because of some uncertainty in this area, the algorithm shown in Fig. 8 is used to ensure use of the appropriate case.

Transfers are simulated for the described system using both schemes. The results are shown in Figs. 12–14. These figures describe the transfer making use of energy storage as "continuous," because this scheme is able to perform transfers without coast periods. The other scheme is labeled "discontinuous," as all transfer segments are performed in sunlight only. Figure 12 compares the radius versus time profiles for both trials. The system not using the available energy storage is at a clear disadvantage, as it takes 40 days longer for it to reach geosynchronous radius.

Figure 13 shows the single segment radius ratio ($\Delta r/r(0)$) with respect to each segment's beginning radius. This information is analogous to a rate of increase. Notable in this plot are the discontinuities found at the end of the traces. These discontinuities are caused by the final transfer segments, where the goal is not to maximize radius, but to achieve the desired GEO radius exactly. Note that the curves cross at a radius of approximately 20,000 km. For lower radii, the scheme using energy storage provides

the largest increase per transfer segment. For radii above this, the scheme not using energy storage provides better results. If we are interested in merely minimizing the transit time, it is a good idea not to use the flywheel-batteries at this point.

Figure 14 compares the propellant use of the two trials. The scheme using energy storage has a clear advantage: Approximately 98 kg of propellant is saved by making use of the spacecraft's energy storage.

Next, we use the spacecraft characteristics from the previous section, but assume that we have an additional 100 kg of system mass that can be used for solar array and battery mass. Our goal is to determine how much of that mass should be used for increasing the size of the solar array, and how much of that mass should be used to increase flywheel-battery capacity.

The previously described spacecraft required 87.5 kg of array mass and 115 kg of battery mass. The spacecraft's initial mass remains at 3000 kg, but we use another 100 kg of this mass for array and battery. First, we look at two extreme cases. One extreme is where we use all of the additional mass for array. Having 100 kg additional solar array provides the spacecraft with more power and higher thrust. With this configuration there is not enough battery storage for continuous thrust through the eclipse as higher altitudes are reached. The other extreme that is chosen is a "pseudo-balanced" configuration. The second-to-last transfer segment requires the most energy storage, if it is to be a transfer with no coast periods. Remember that the last transfer segment is typically a correction, that we assume to be small for this approximation. Approximating the last transfer segment as a circular orbit at GEO, and using Eqs. 22 and 23, we find that 56.75 kg of the additional mass should be used for flywheel-battery mass, and the remaining additional mass should be used for the solar array.

These two spacecraft configurations are compared, with the results are illustrated in Figs. 15 and 16. Figure 15 illustrates orbital radius versus time for both con-

figurations. The solid curve represents the configuration where all additional mass is used for increased array size, which is labeled "array only." The dotted curve is for the "pseudo-balanced" configuration. The configuration where only array mass is added clearly has an advantage in minimizing transit time, as it arrives at a geosynchronous radius 54 days before the other configuration does. This configuration takes 946 transfer segments and 128 days, while the "pseudo-balanced" configuration takes 1355 revolutions and 182 days. Figure 16 shows the mass versus radius curves for the two configurations. The "pseudo-balanced" configuration saves merely 12 kg of mass, so Fig. 16 appears to have only one trace.

It can be argued that these results do not give a complete picture, because we do not have any indication of the behavior that will be exhibited between these two extreme cases. In Ref. 14, several intermediate cases are presented, and the trend is clear. Though the use of additional energy storage does increase efficiency, it also increases the time to achieve the orbit transfer.

Conclusions

Energy storage has previously been thought inappropriate for use in solar electric propulsion applications. When optimal transfers are considered, along with the high energy densities that flywheel energy storage may eventually provide, the combination of solar electric propulsion and flywheel energy storage may offer improved performance. Because the fraction of the orbital period spent in eclipse increases as orbit radius increases, storing energy for use during eclipse increases the time it takes to perform a transfer to geosynchronous orbit. However, the increase in time of flight is countered by an increase in payload mass delivered to geosynchronous altitude. Furthermore, most satellites require energy storage for the primary mission, so that the mass of the energy storage system is not a penalty.

Acknowledgments

This work was supported by Charles Donet of the Air Force Research Laboratory and by Arje Nachman of the Air Force Office of Scientific Research.

References

[1] Kechichian, J. A., "Orbit Raising with Low-Thrust Tangential Acceleration in Presence of Earth Shadow," *Journal of Spacecraft and Rockets*, Vol. 35, No. 4, 1998, pp. 516–525.

[2] Kluever, C. A. and Oleson, S. R., "Direct Approach for Computing Near-Optimal Low-Thrust Earth-Orbit Transfers," *Journal of Spacecraft and Rockets*, Vol. 35, No. 4, 1998, pp. 509–515.

[3] Free, B. A., "North-South Stationkeeping with Electric Propulsion using Onboard Battery Power," COMSAT Laboratories, Clarksburg, Maryland, 1980.

[4] Avila, E. R., "Parametric Studies and Orbital Analysis for an Electric Orbit Transfer Vehicle Space Flight Demonstration," in L. J. Wood, S. J. Kerridge, R. G. Melton, and R. C. Thompson (editors), *Proceedings of the American Astronautical Society/AIAA Space Flight Mechanics Meeting*, Pasadena, California, February 22–24, 1993, pp. 1215–1240.

[5] Fitzgerald, A. M., "Impact of Energy Storage System Mass on the Performance of Orbit Transfer Vehicles Using Solar Electric Propulsion," in A. W. Adam and R. C. Winn (editors), *Proceedings of the 29th Intersociety Energy Conversion Engineering Conference*, Monterey, California, August 7–11, 1994, pp. 316–319.

[6] Hearth, D. P. (editor), *A Forecast of Space Technology: 1980–2000*, Number NASA SP-387. Washington, D. C., 1976.

[7] McKay, M. F., McKay, D. S., and Duke, M. B. (editors), *Space Resources: Energy, Power, and Transport*, Number NASA SP-509, Volume 2. Houston, 1992.

[8] Hall, C. D., "High-Speed Flywheels for Integrated Power Storage and Attitude Control," in N. A. Kheir (editor), *Proceedings of the 1997 American Control Conference*, Albuquerque, New Mexico, June 4–6, 1997, pp. 1894–1898.

[9] Christopher, D. A. and Beach, R., "Flywheel Technology Development Program for Aerospace Applications," in B. Moore (editor), *Proceedings of the 1997 National Aerospace and Electronics Conference*, Dayton, Ohio, July 14–18, 1997, pp. 602–608.

[10] Havenhill, D., Robinson, W., Hanks, J., Gisler, G., Spina, L., and Ginter, S., "Spacecraft Energy Storage Systems," in B. Moore (editor), *Proceedings of the 1997 National Aerospace and Electronics Conference*, Dayton, Ohio, July 14–18, 1997, pp. 609–616.

[11] Thorne, J. D. and Hall, C. D., "Approximate Initial Lagrange Costates for Continuous Thrust Spacecraft," *Journal of Guidance, Control and Dynamics*, Vol. 19, No. 2, 1996, pp. 283–288.

[12] Thorne, J. D. and Hall, C. D., "Minimum-Time Continuous-Thrust Orbit Transfers," *Journal of the Astronautical Sciences*, Vol. 45, No. 4, 1997, pp. 411–432.

[13] Neta, B. and Vallado, D., "On Satellite Umbra/Penumbra Entry and Exit Positions," *Journal of the Astronautical Sciences*, Vol. 48, No. 1, 1998, pp. 91–104.

[14] Marasch, M. W. Applying Flywheel Energy Storage to Solar Electric Orbital Transfers. Master's thesis, Graduate School of Engineering, Air Force Institute of Technology, Wright-Patterson AFB, Ohio, December 1997.

Table 1: Circle-to-circle boundary value problem

Initial Conditions (Canonical Units)	Final Conditions (Canonical Units)
$r(0) = 1$	$r(t_f) = R$
$u(0) = 0$	$u(t_f) = 0$
$v(0) = 1$	$v(t_f) = \sqrt{1/R}$
$\lambda_r(0) = 1$	
$\lambda_u(0) = ?$	$t_f = ?$
$\lambda_v(0) = ?$	

Figure Captions

Fig. 1. Optimal transfer geometry in polar coordinates.

Fig. 2. Simplified shadow geometry in the ecliptic plane.

Fig. 3. Optimal circle-to-circle transfer.

Fig. 4. Maximum transfer accomplished while in sunlight.

Fig. 5. Orbital transfer segment with a low level of energy storage.

Fig. 6. Orbital transfer without a coast phase.

Fig. 7. Algorithm for simulating a large orbital transfer.

Fig. 8. Algorithm for determining appropriate case.

Fig. 9. Radius versus time for two spacecraft configurations.

Fig. 10. Radius versus time for the first 15 days.

Fig. 11. Spacecraft mass remaining with respect to radius achieved.

Fig. 12. Radius versus time comparison for two transfer schemes.

Fig. 13. Radius increase ratios versus radius comparison.

Fig. 14. Spacecraft mass versus radius comparison.

Fig. 15. Radius versus time for two extreme configurations.

Fig. 16. Mass remaining versus radius for two extreme configurations.

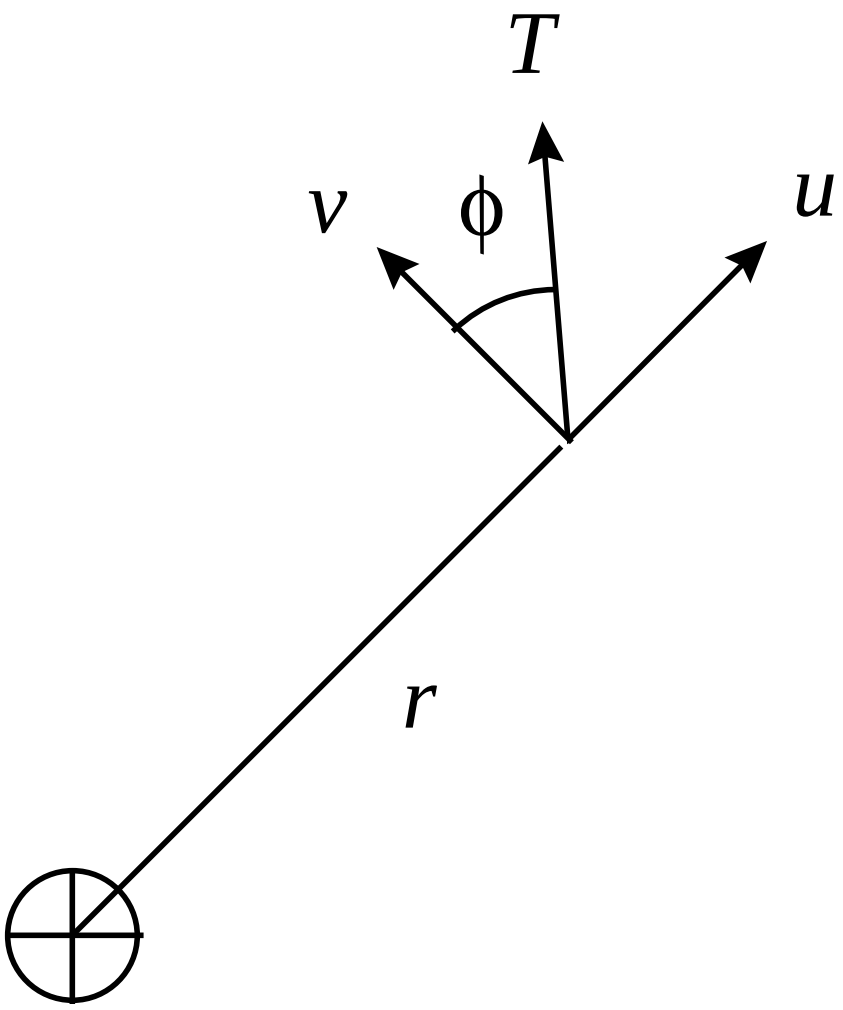

Figure 1. Optimal transfer geometry in polar coordinates.

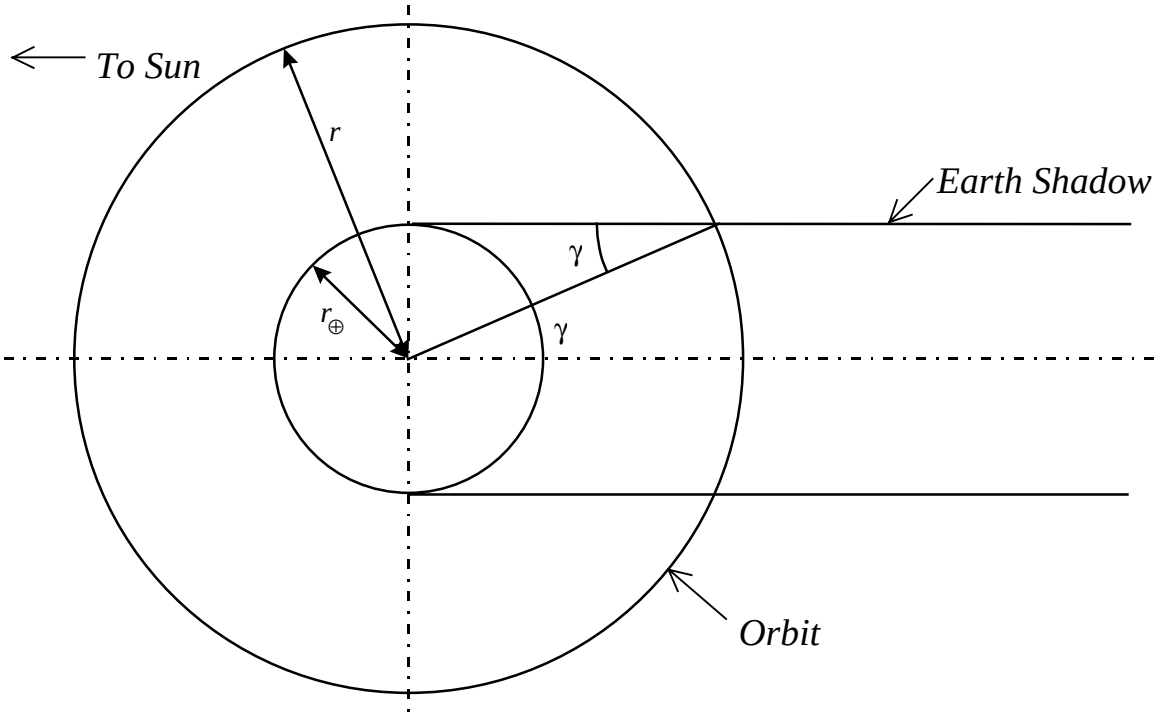

Figure 2. Simplified shadow geometry in the ecliptic plane.

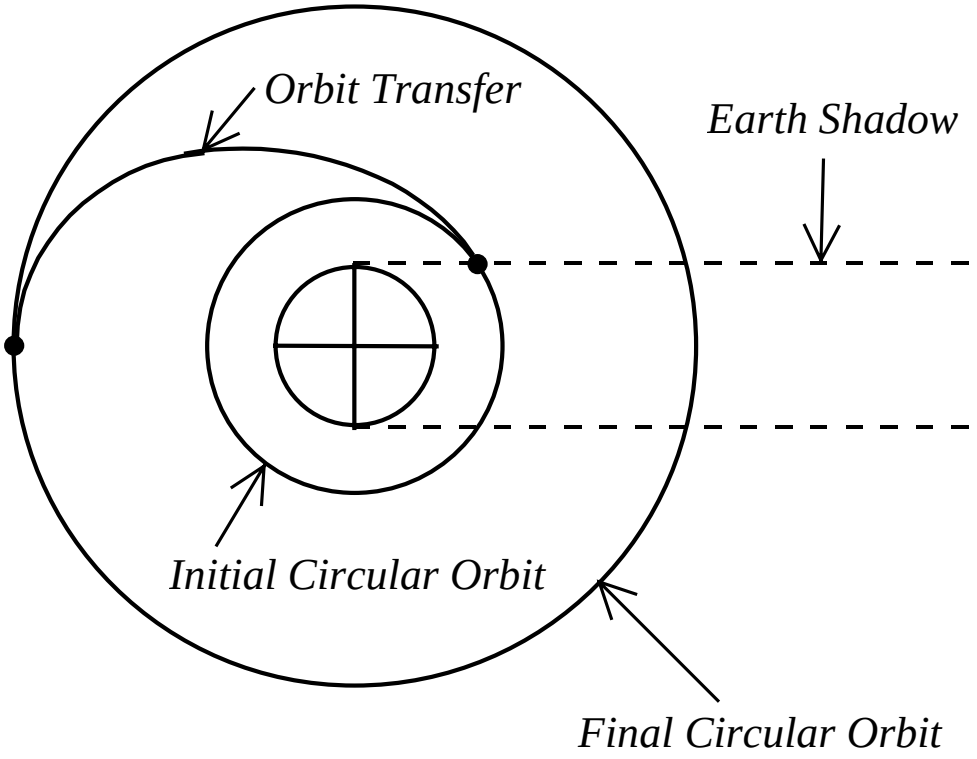

Figure 3. Optimal circle-to-circle transfer.

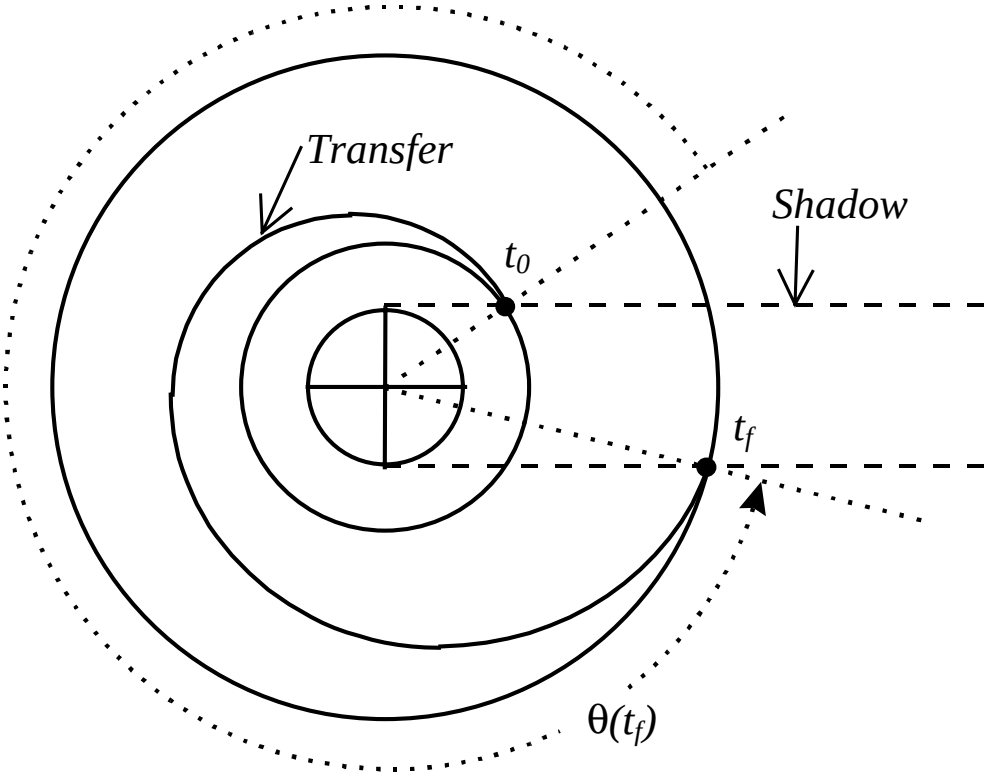

Figure 4. Maximum transfer accomplished while in sunlight.

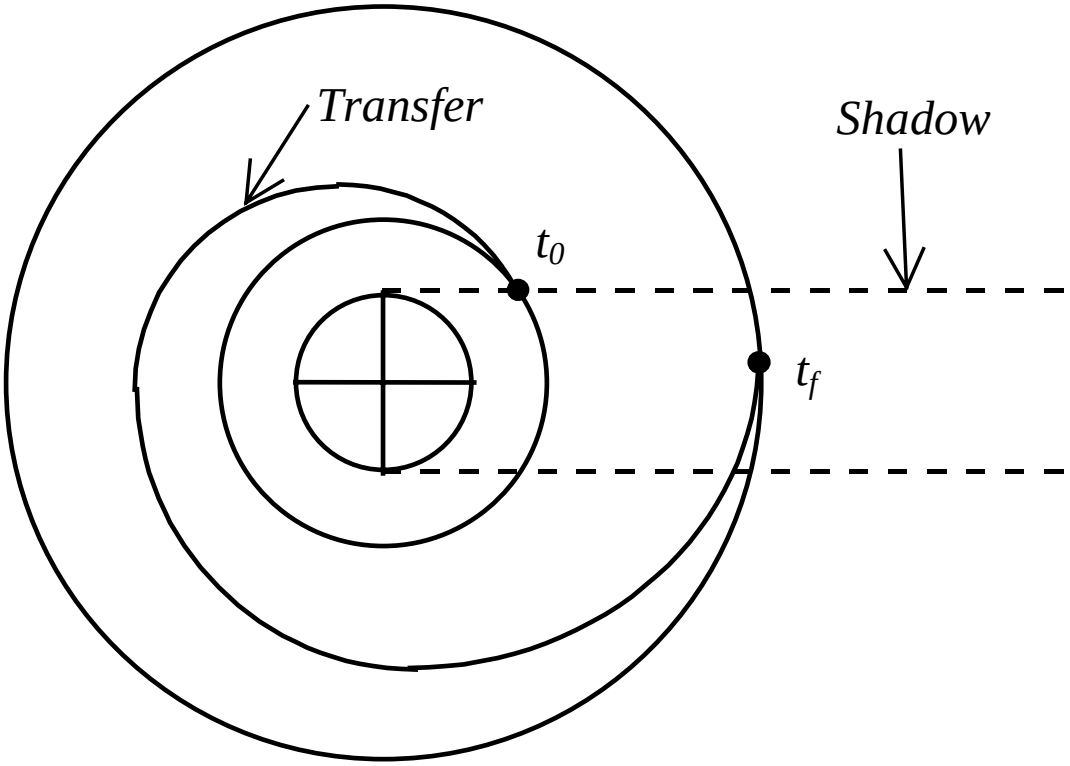

Figure 5. Orbital transfer segment with a low level of energy storage.

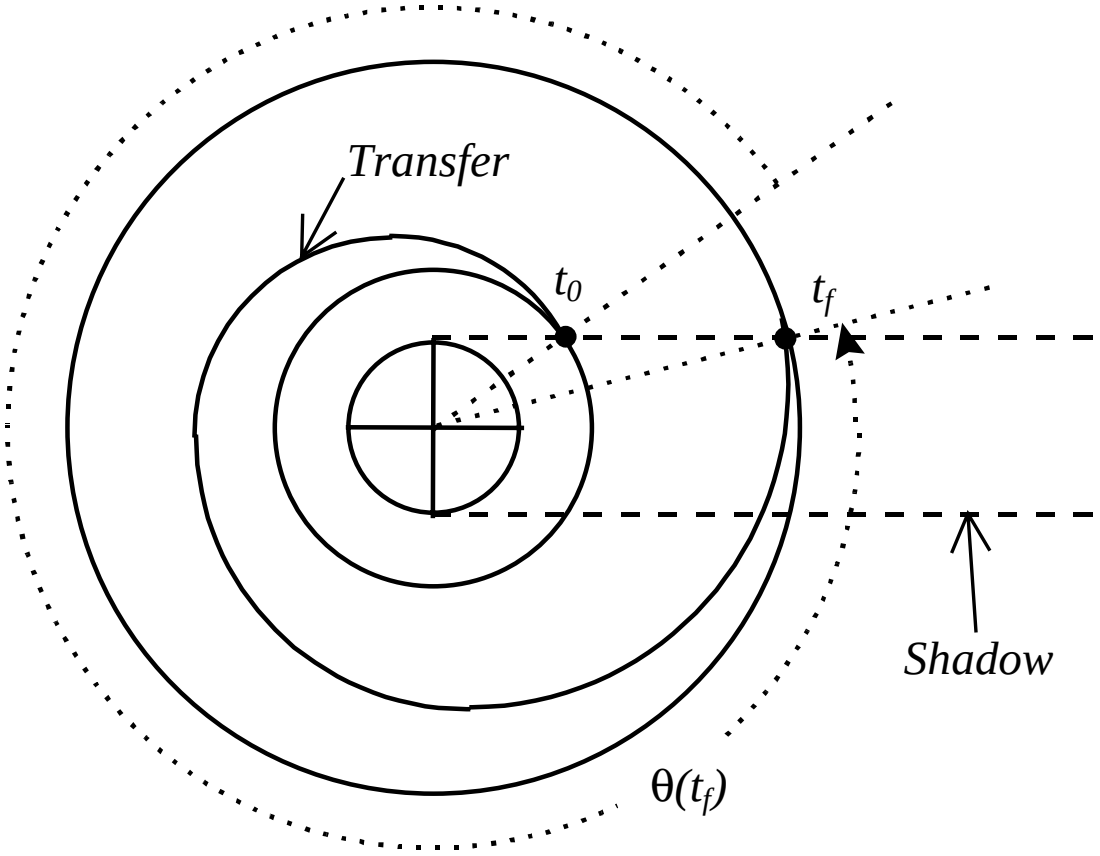

Figure 6. Orbital transfer without a coast phase.

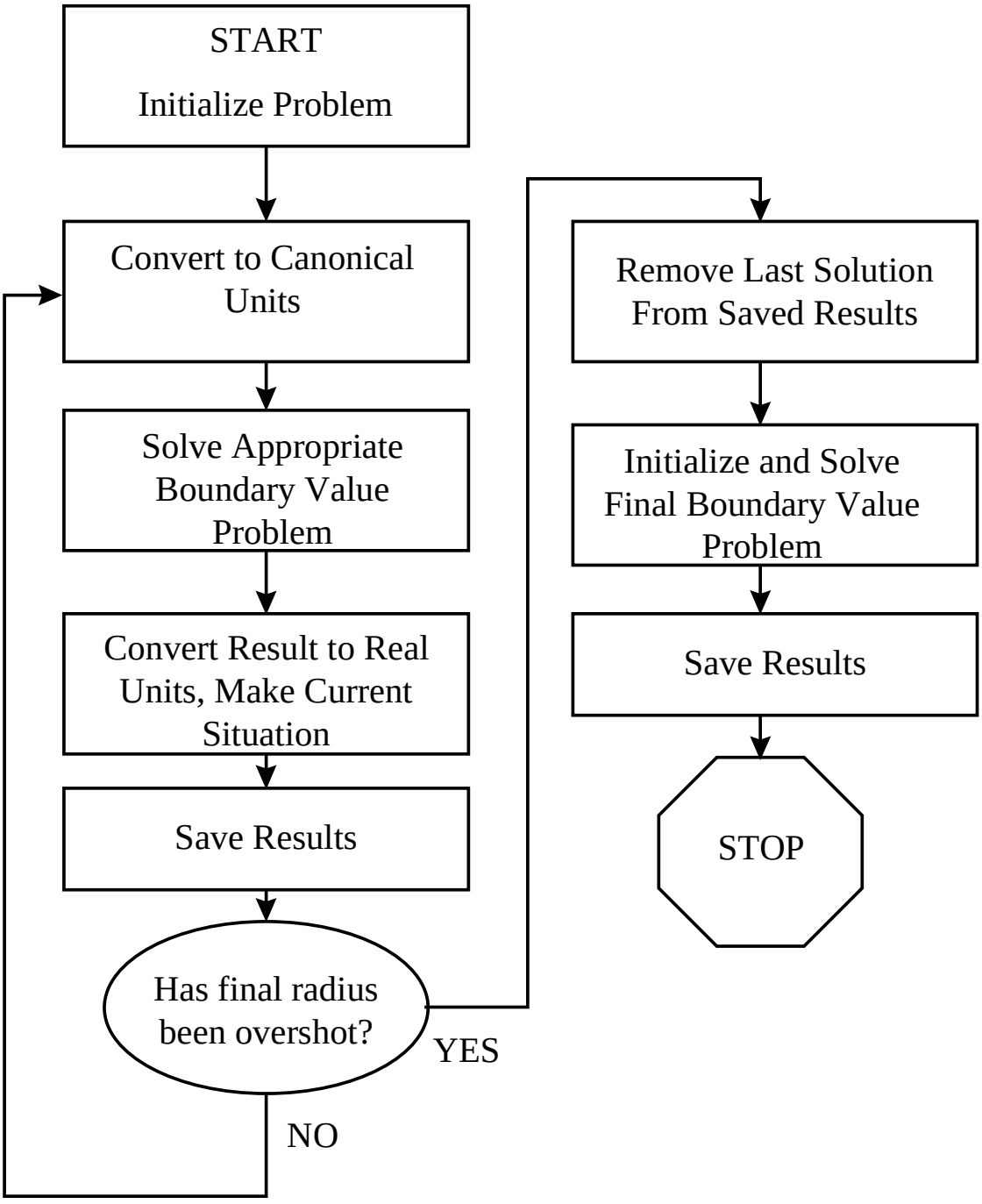

Figure 7. Algorithm for simulating a large orbital transfer.

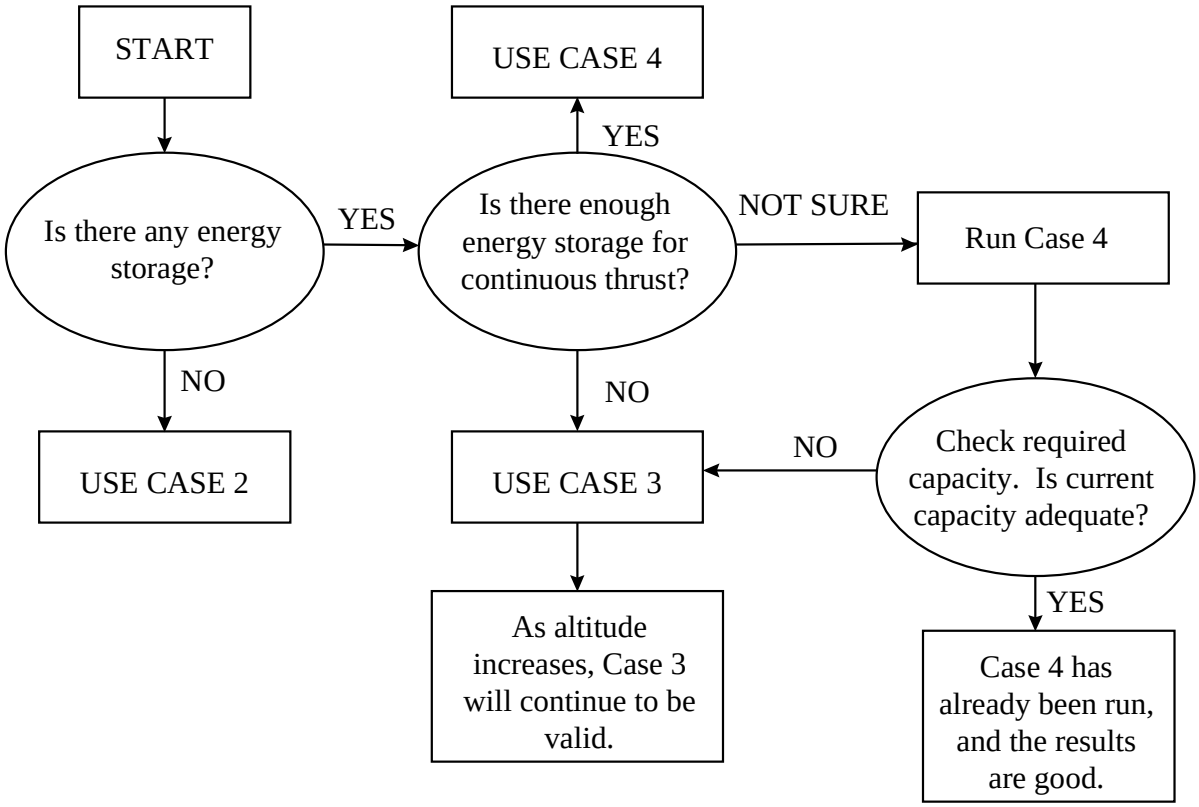

Figure 8. Algorithm for determining appropriate case.

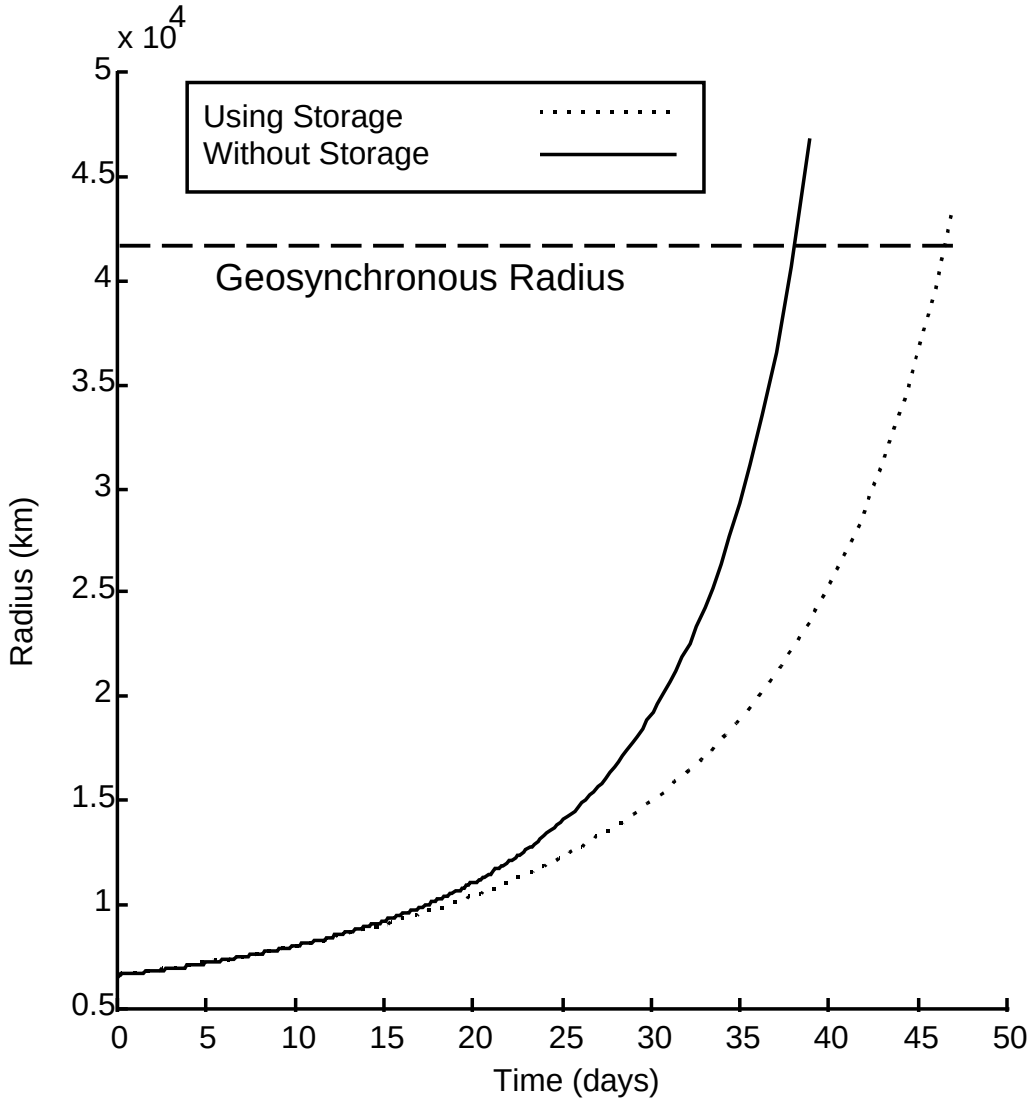

Figure 9. Radius versus time for two spacecraft configurations.

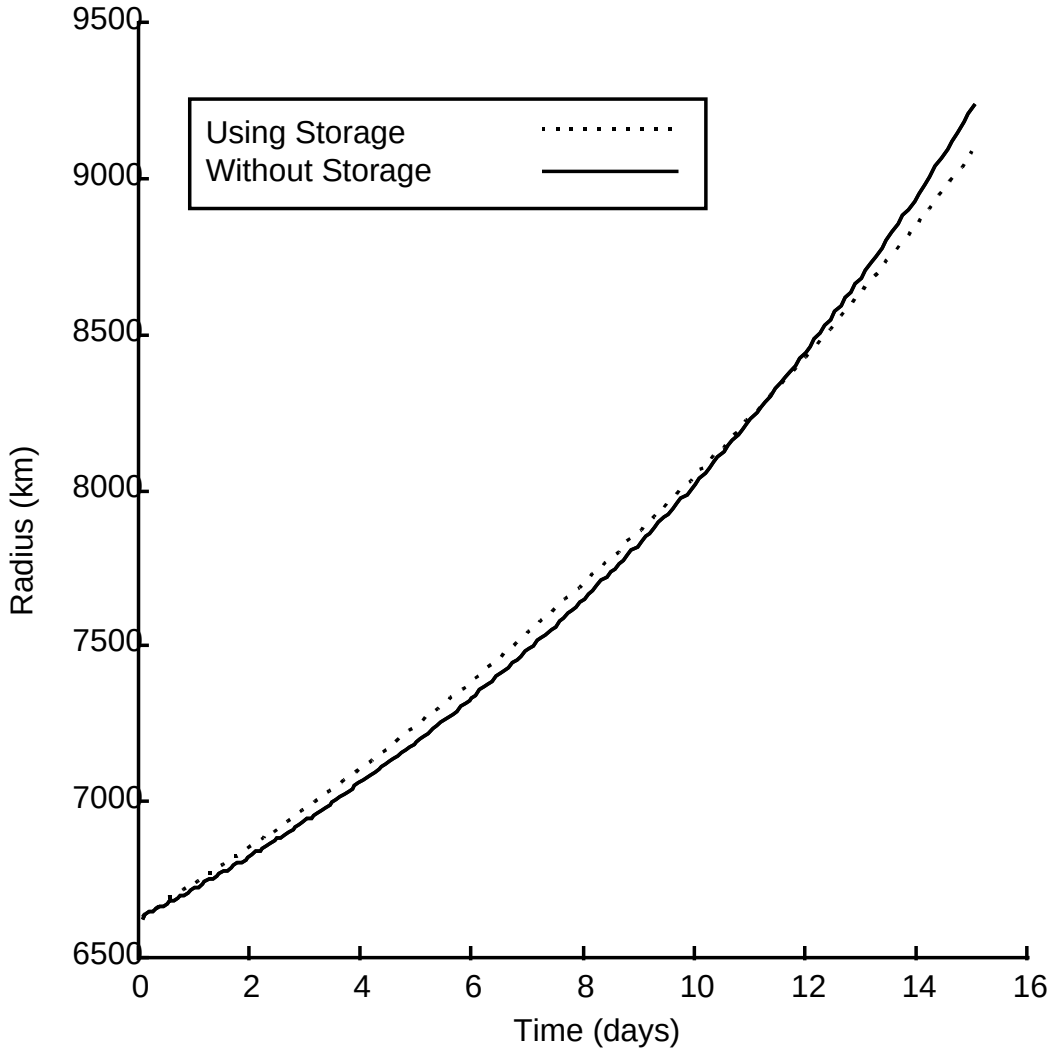

Figure 10. Radius versus time for the first 15 days.

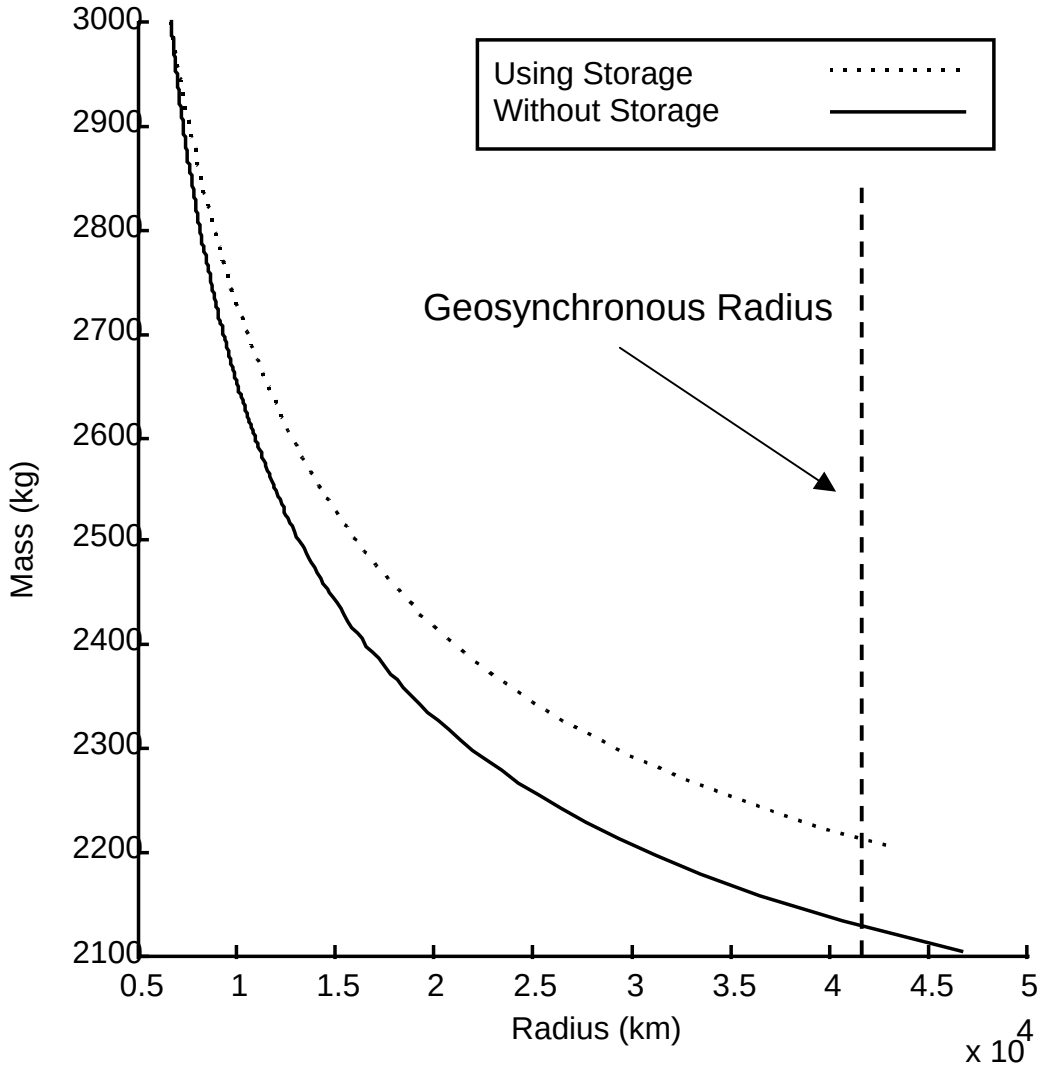

Figure 11. Spacecraft mass remaining with respect to radius achieved.

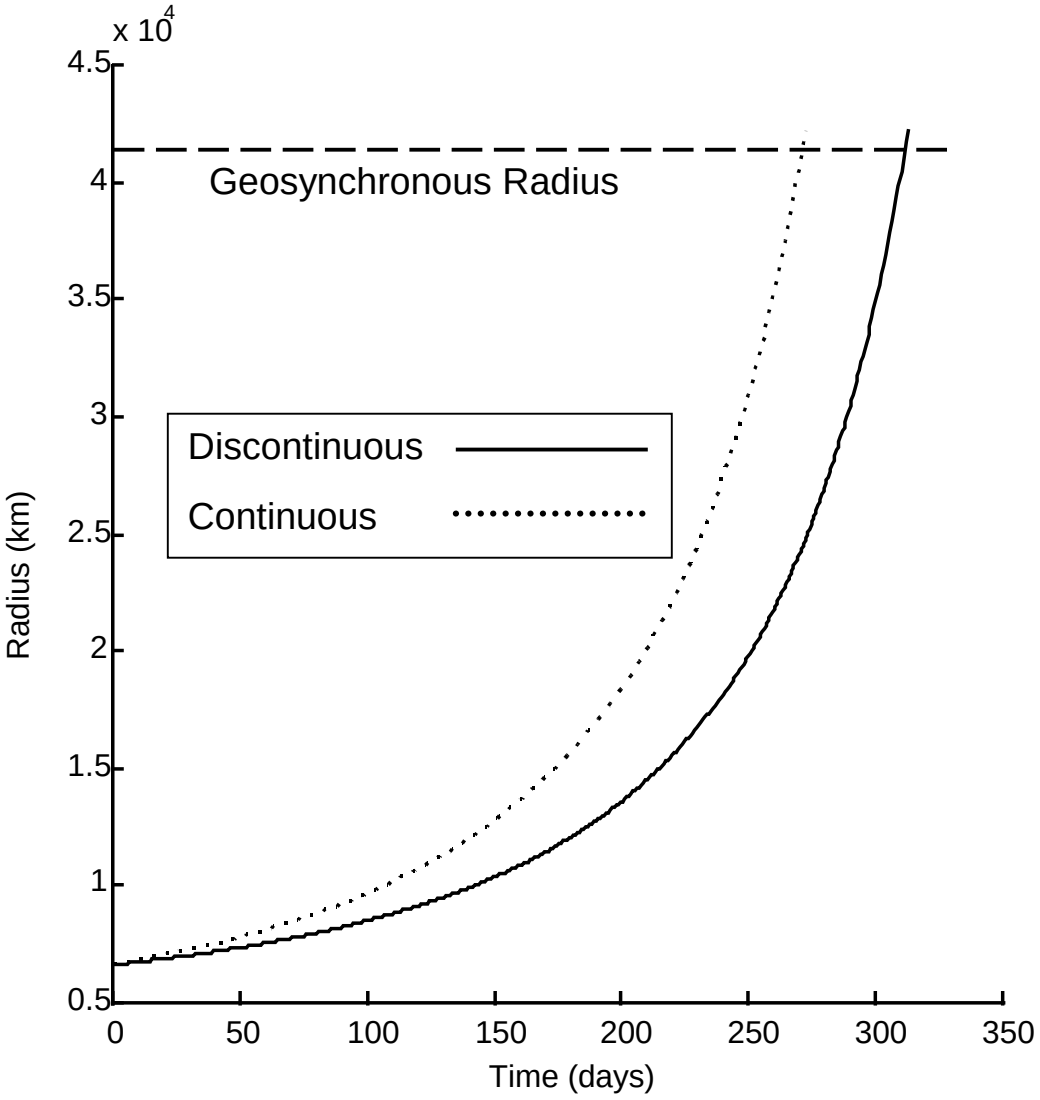

Figure 12. Radius versus time comparison for two transfer schemes.

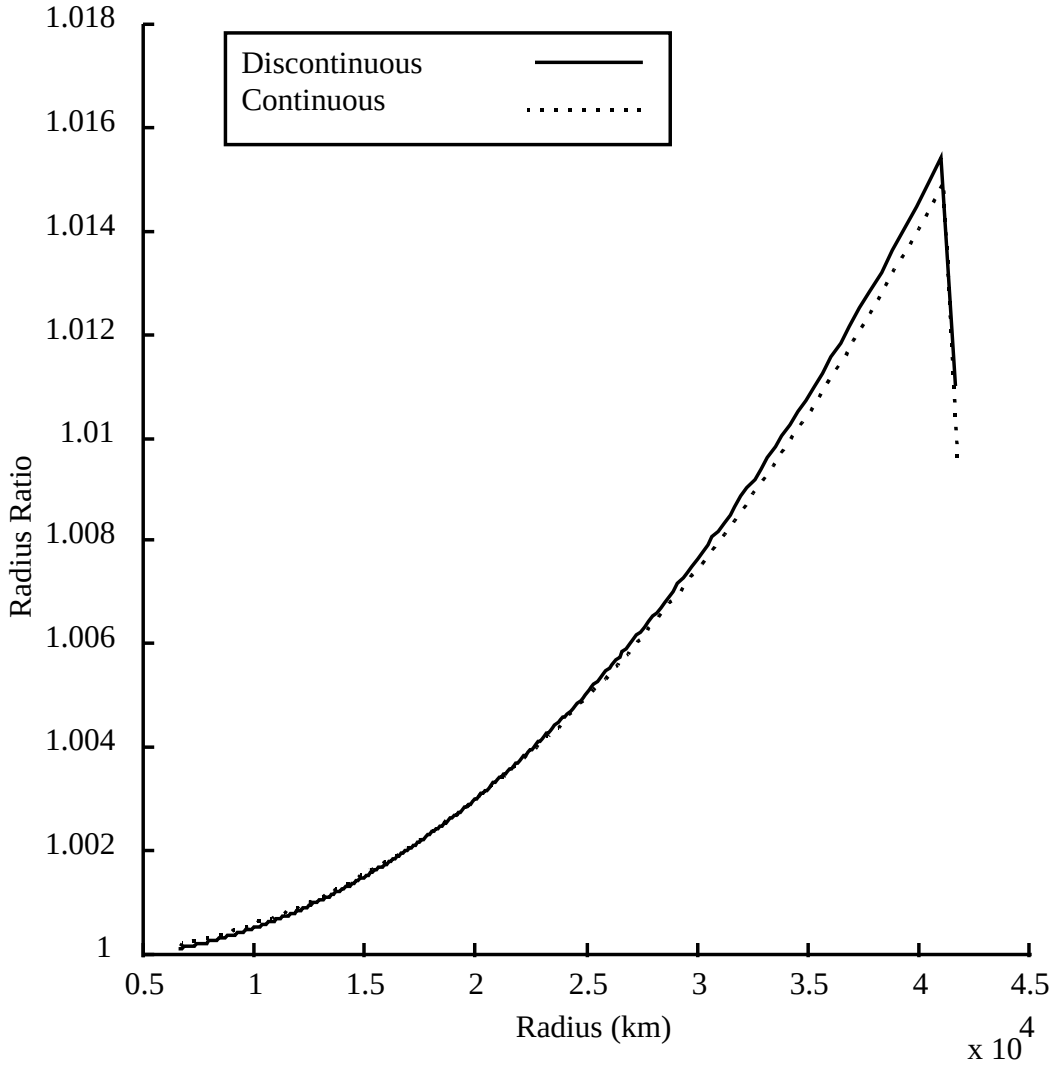

Figure 13. Radius increase ratios versus radius comparison.

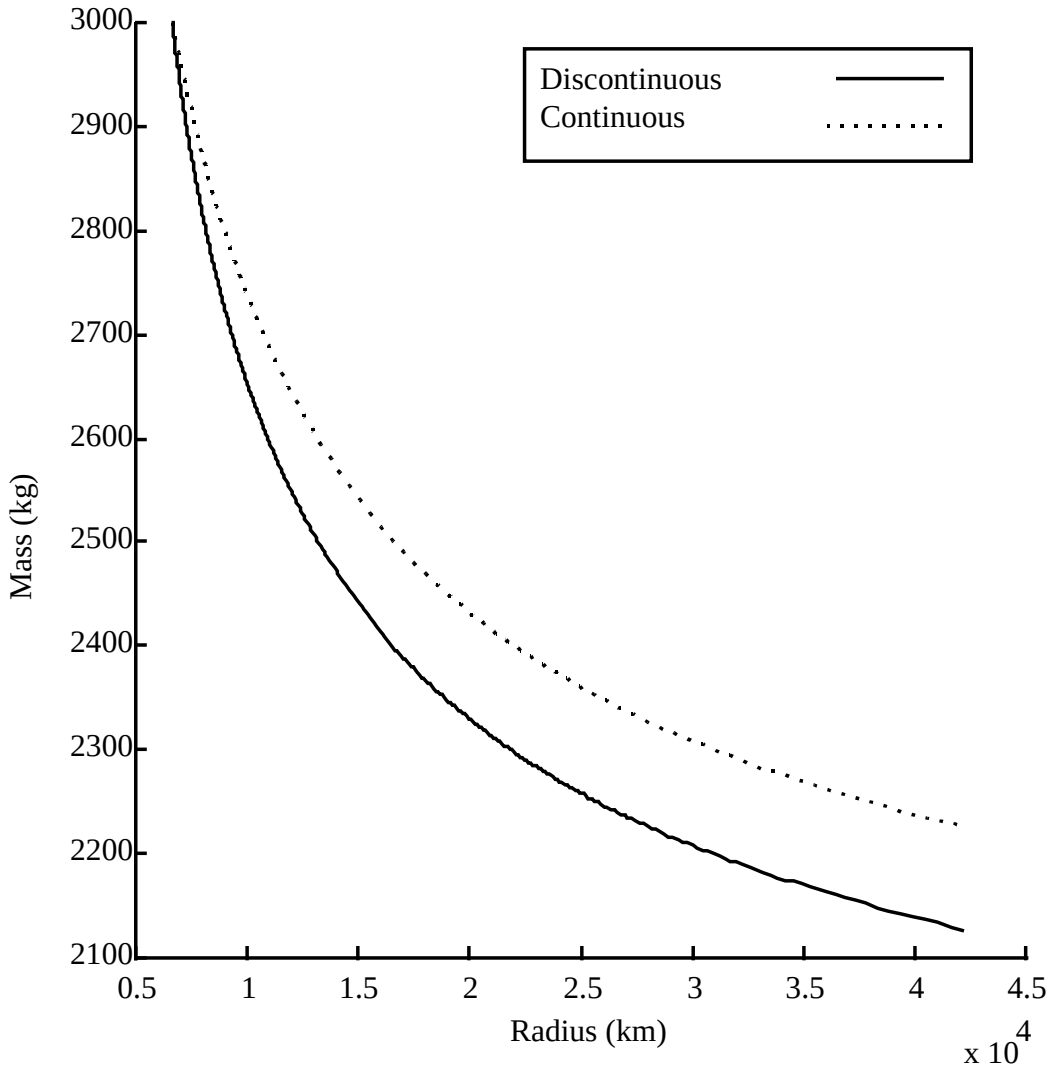

Figure 14. Spacecraft mass versus radius comparison.

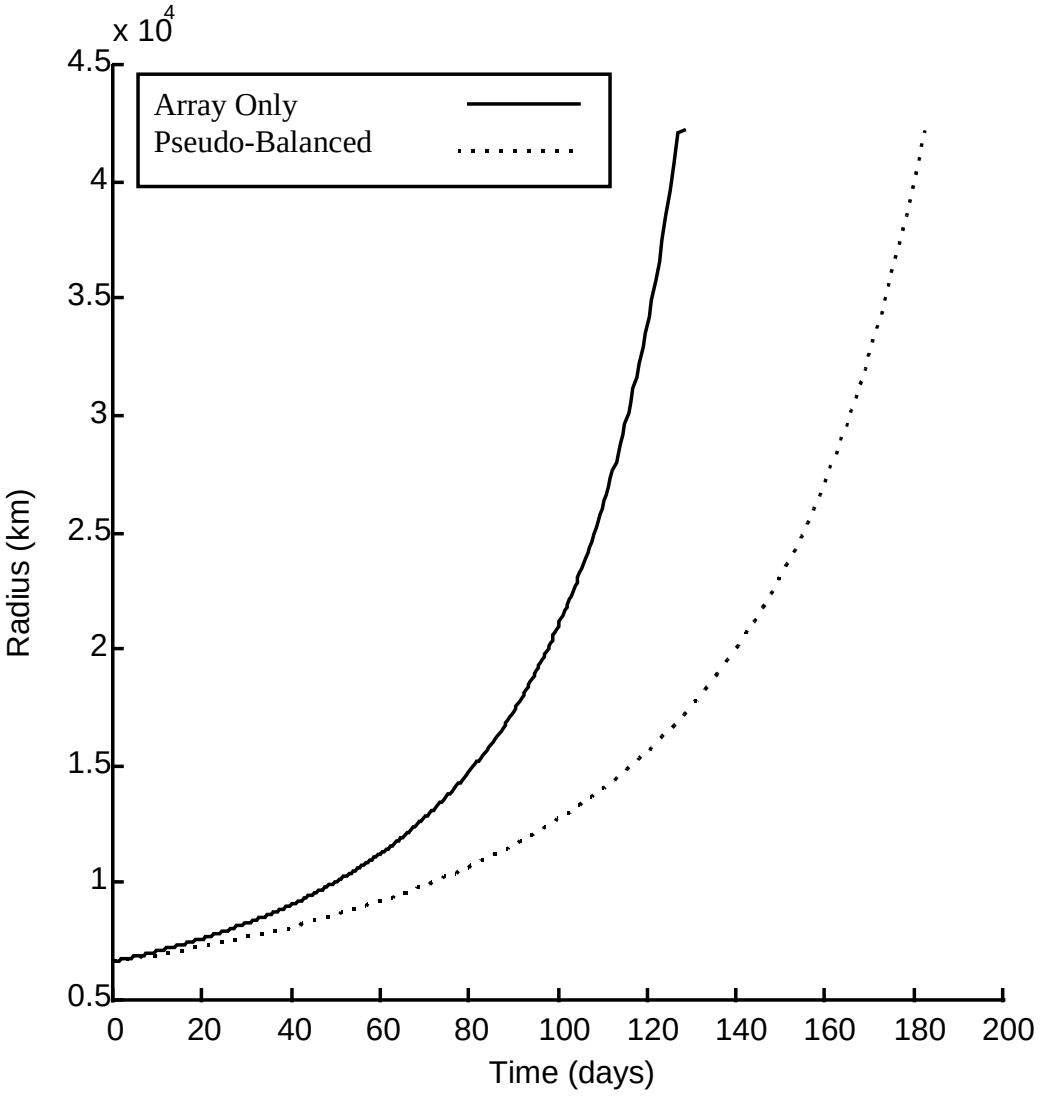

Figure 15. Radius versus time for two extreme configurations.

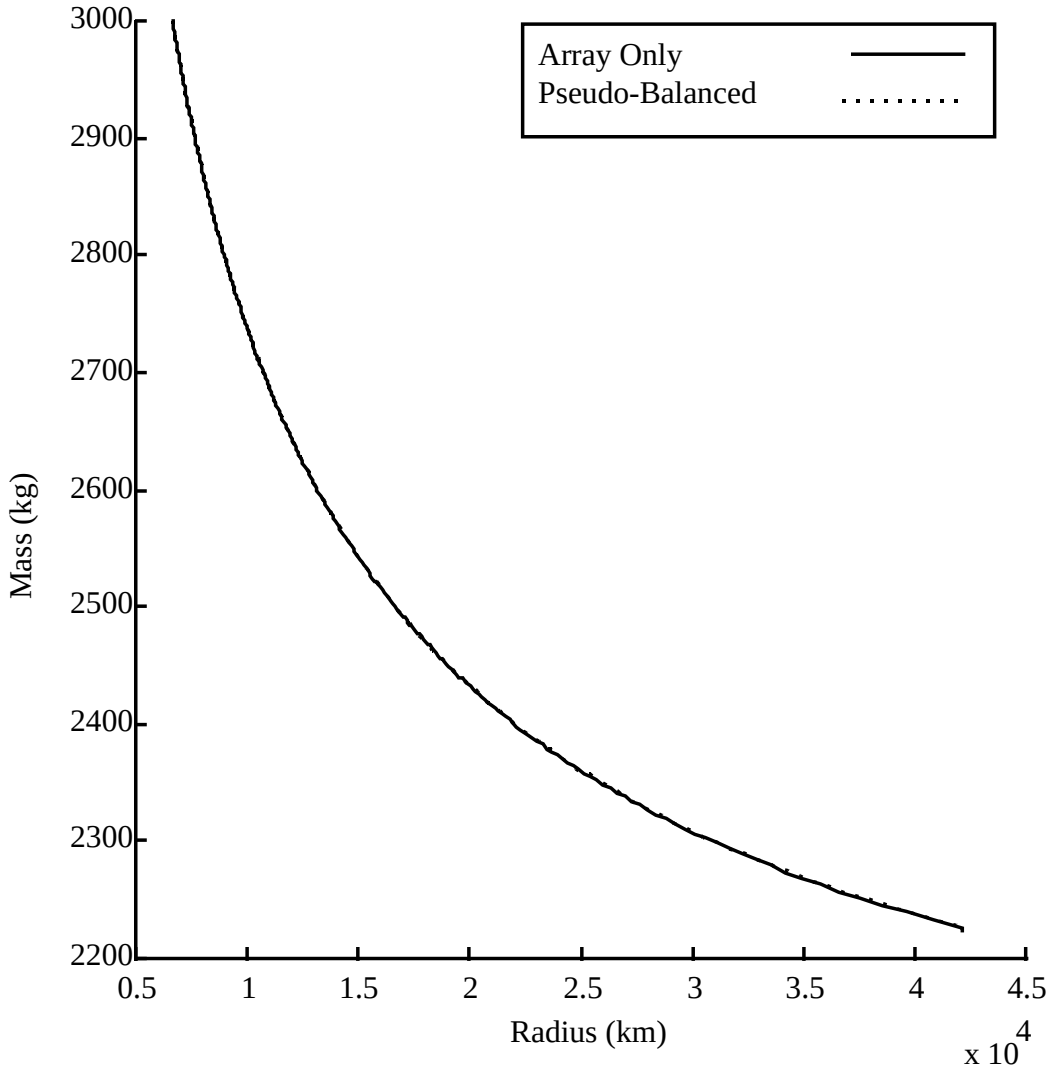

Figure 16. Spacecraft mass remaining versus radius for two extreme configurations.